

Spacing distribution in the 2D Coulomb gas: Surmise and symmetry classes of non-Hermitian random matrices at non-integer β

Gernot Akemann,^{1,*} Adam Mielke,^{2,†} and Patricia Pakler^{1,‡}

¹*Faculty of Physics, Bielefeld University, Postfach 100131, 33501 Bielefeld, Germany*

²*Technical University of Denmark, asmussens Alle, Building 303B, 2800 Kgs. Lyngby, Denmark*

(Dated: April 2, 2022)

A random matrix representation is proposed for the two-dimensional (2D) Coulomb gas at inverse temperature β . For 2×2 matrices with Gaussian distribution this yields a surmise for the nearest neighbour spacing distribution of complex eigenvalues in radial distance. It reproduces the 2D Poisson distribution at $\beta = 0$ and approximates the complex Ginibre ensemble at $\beta = 2$. The surmise is used to fit data from open quantum spin chains and ecology. The spacing distributions of complex symmetric and complex quaternion self-dual ensembles are fitted by *non-integer values* $\beta = 1.4$ and $\beta = 2.6$, respectively. They have been suggested as the only two symmetry classes with 2D bulk statistics different from the Ginibre ensemble.

Introduction. The description of the spacing between neighbouring energy levels by the distribution following from the three Wigner-Dyson classes of random matrices is probably the most used quantity in this field. A simple, approximate formula exists, the Wigner surmise, that following the Bohigas-Giannoni-Schmit conjecture [1, 2] applies to fully chaotic quantum Hamiltonians. The symmetry class depends on the presence or absence of time-reversal and spin taking integer or half-integer values, Dyson’s threefold way [3]. This approach owes its universality to a link to a Coulomb gas description confined to a line, the Dyson gas. Many applications beyond quantum chaos exist, and we refer to [4, 5] for references.

The idea to describe many-body chaotic quantum systems using Hermitian random matrices goes back to the concept of the compound nucleus by Bohr, see [4] for a historic account. While the consideration of non-Hermitian random matrices with complex spectra was initially born out of mathematical curiosity [6], nowadays there are many applications to non-Hermitian operators with a two-dimensional (2D) spectrum. Examples include localisation in 2D random Schrodinger operators [7], dissipative quantum systems [8], random neural networks [9], quantum field theory with a quark chemical potential [10], and beyond physics in the adjacency matrix of directed complex networks [11] or ecology [12]. In particular open chaotic quantum system have seen much activity recently, where the effect of integrability vs. chaos is studied in spin chains [13–15] or the kicked rotor [16]. Apart from these applications the 2D Coulomb gas (2DCG) is fascinating in its own right as a statistical mechanics problem, cf. [17], displaying the phenomenon of crystallisation [18, 19], see [20] for recent numerics and [21] for a mathematical physics perspective.

As in 1D, the simplest null models proposed to describe spectra in 2D are Poisson random variables for completely uncorrelated points, and complex eigenvalues of non-Hermitian random matrices for strong correlations based on symmetry. The conjectured correspondence to quantum integrable respectively chaotic systems has been

extended to 2D [8]. In particular, it was argued based on perturbation theory [8, 22] that the nearest neighbour spacing in radial distance in 2D is universal at small distance and displays a cubic level repulsion, irrespectively of time-reversal being preserved or not [23].

Perhaps surprisingly, the spacing distribution in the three non-Hermitian Ginibre ensembles all agree in the bulk of the spectrum away from the real axis [8, 13, 24]. This is in stark contrast to the three Hermitian Wigner-Dyson classes where the matrices with real, complex or quaternion elements display a different level repulsion, governed by the respective inverse temperature $\beta = 1, 2, 4$ of the Dyson gas. Is there more than a single symmetry classes in the bulk in 2D and is there a simple formula describing these? In 1D, Dyson’s classification [3] was extended to 10 classes by Altland and Zirnbauer [25]. However, this did not extend the 3 classes of local bulk statistics, as additional symmetries only manifest themselves at specific points of the spectrum. Likewise, based on the symmetry classes of Dirac operators [26], a classification of non-Hermitian random matrices was undertaken [27], that was recently revisited [28] and leads to 38 classes. Based on heuristic arguments and numerics it was found that also here only three distinct classes of 2D bulk statistics exist [14]: The Ginibre ensemble [6] and two further classes labelled AI^\dagger and AII^\dagger (in analogy to [25]), that possess additional symmetries under transposition. They are respectively given by complex symmetric and complex quaternion self-dual matrices [14] (related to complex antisymmetric matrices [29]). The spectral statistics of AI^\dagger was found in the complex spectrum of the kicked rotor [16], where a transition from time-reversal invariance in AI^\dagger and its breaking toward the Ginibre ensemble was observed. All three classes were found in the spectrum of Liouville operators of dissipative quantum spin chains, subject to certain external fields [14], and in non-Hermitian Dirac operators in quantum field theories [30]. For questions of dynamics and non-equilibrium of Liouville operators and a comparison of their global statistics to non-Hermitian random matrices see [31–34].

It is the goal of this article to find an approximate description of the spacing distribution of these 3 classes in terms of a 2DCG at inverse temperature β . Furthermore, a simple formula or surmise will allow us to describe the transition to 2D Poisson at $\beta = 0$. This is in contrast to 1D, where Wigner's surmise

$$p_{\text{Wigner}}^{\text{1D}}(s) = a_\beta s^\beta \exp[-b_\beta s^2], \quad (1)$$

with $b_\beta = \Gamma[(\beta+2)/2]^2 / \Gamma[(\beta+1)/2]^2$ and $a_\beta = 2b_\beta^{(\beta+1)/2}$, works very well at increasing values of $\beta = 1, 2, 4$, but fails closer to Poisson in 1D $p_{\text{Poisson}}^{\text{1D}}(s) = \exp[-s]$, corresponding to $\beta = 0$. Several phenomenological interpolations between $\beta = 0$ and 1 exist, cf. [4]. More recently, a 2×2 invariant matrix representation of the 1D Dyson gas for $\beta \in [0, 2]$ has been used to derive an integral representation [35]. We will follow this approach and extend it to a 2DCG at $\beta \geq 0$ also called non-Hermitian β -ensemble, staying well below the crystallisation transition.

The local statistics in β -ensembles is a very active field in mathematical physics, see [21] for a review on 2D. Even in 1D in the bulk, where there is a limiting point process in terms of a stochastic operator, the sine- β process [37], no explicit expression is known for the spacing distribution. In 2D closed form expressions for the local statistics exist only for the spacing in 2D for Poisson ($\beta = 0$) and the complex Ginibre ensemble (GinUE) at $\beta = 2$, see (10) below. Consequently, a detailed comparison to the spacing in the intermediate regime previously relied on numerical simulations of the 2DCG, cf. [13]. When comparing to data, also in 2D spectra have to be unfolded which is quite nontrivial, see [10, 13, 22]. For that reason, complex valued ratios between nearest and next-to-nearest neighbour spacings have been proposed as an alternative [38].

Invariant Non-Hermitian β -Ensemble. We begin by defining the joint density of points (charges) of the 2DCG at fixed inverse temperature $\beta > 0$, subject to a confining potential V

$$\mathcal{P}_{\beta,N}(z_1, \dots, z_N) \propto e^{\beta \sum_{i>j} \log |z_i - z_j| - \sum_{i=1}^N V(z_i, z_i^*)}. \quad (2)$$

In order to be able to take the limit $\beta \rightarrow 0$ of uncorrelated points, cf. [39], we have rescaled the potential to remove its dependence on β . An explicit random matrix representation is only known for $\beta = 2$, given by the complex eigenvalue distribution of the GinUE [6] with Gaussian potential $V(z, z^*) = |z|^2$. Assuming that the bulk of the spectrum is translation invariant, we can compute the nearest neighbour spacing distribution in 2D by putting a point at the origin and compute the probability to find the next point at radial distance s ,

$$p_{\beta,N}(s) \propto \prod_{j=2}^N \int_{\mathbb{C}} d^2 z_j \mathcal{P}_{\beta,N}(0, z_2, \dots, z_N) \delta(|z_2| - s). \quad (3)$$

For $\beta = 2$ this expression can be computed analytically as given in (10), see [8, 40] for a derivation.

Let us construct an ensemble of $N \times N$ complex normal non-Hermitian random matrices $J \neq J^\dagger$, with $[J, J^\dagger] = 0$, that has the same joint distribution of complex eigenvalues as the 2DCG (2) for arbitrary $\beta > 0$. Following [40, Chapt. 15] the Vandermonde determinant $\Delta_N(Z) = \prod_{i>j}^N (z_i - z_j)$ of complex eigenvalues of J , that provides the logarithmic Coulomb interaction in (2), can be written as follows

$$|\Delta_N(Z)|^2 = \left| \det_{1 \leq i, j \leq N} [z_i^{j-1}] \right|^2 = \det_{1 \leq i, j \leq N} [\text{Tr}(J^{i-1} J^{\dagger j-1})] \quad (4)$$

where we used $|\det[A]|^2 = \det[AA^\dagger]$ and replaced the sums in $(AA^\dagger)_{i,j}$ as $\sum_{k=1}^N z_k^{i-1} z_k^{*j-1} = \text{Tr}(J^{i-1} J^{\dagger j-1})$. Because the Jacobian for the diagonalisation of complex normal matrices $J = UZU^\dagger$, with $U \in U(N)$ and $Z = \text{diag}(z_1, \dots, z_N)$, is known [41] to be proportional to $|\Delta_N(Z)|^2$, we obtain from the following distribution

$$\begin{aligned} \mathcal{P}_{\beta,N}(J) &\propto \frac{\exp[-\text{Tr} V(J, J^\dagger)]}{\det_{1 \leq i, j \leq N} [\text{Tr}(J^{i-1} J^{\dagger j-1})]^\eta} \\ &\propto |\Delta_N(Z)|^{2-2\eta} e^{-\sum_{i=1}^N V(z_i, z_i^*)}, \end{aligned} \quad (5)$$

of a non-Hermitian β -ensemble. It agrees with (2) when identifying $\beta = 2 - 2\eta$. The integrals converge for $\beta \geq 0$ or $\eta \leq 1$ (however, cf. [39] when $\beta = 2c/N$ for $c > -2$). This allows us to interpolate between the Poisson point process at $\beta = 0$ and the GinUE at $\beta = 2$, or larger values of β , when making $\eta < 0$. Although this β -ensemble (5) is invariant and well defined for any N , we have so far only been able to obtain analytical results for $N = 2$ with $V(J, J^\dagger) = JJ^\dagger$ Gaussian, following [35] closely.

Using the standard parametrisation of complex normal matrices at $N = 2$, and the simple resulting form of the denominator $[2\text{Tr}(JJ^\dagger) - \text{Tr} J \text{Tr} J^\dagger]^\eta$, allows us to obtain the normalised joint distribution of matrix elements (see [42]) and of complex eigenvalues with V Gaussian,

$$\mathcal{P}_{\beta,N=2}(z_1, z_2) = K_\beta |z_2 - z_1|^\beta \exp[-|z_1|^2 - |z_2|^2], \quad (6)$$

where $K_\beta^{-1} = \pi^2 2^{\beta/2} \Gamma[1 + \beta/2]$ [42]. Apart from being able to determine the spectral density, our main interest here is its spacing distribution $p_{\beta,2}(s)$. Assuming translational invariance (justified in [42]), as in (3) we condition $z_1 = 0$ to be at the origin and calculate the probability that the second eigenvalue z_2 is at radial distance s ,

$$p_{\beta,2}(s) = 2\pi K_\beta s^{1+\beta} e^{-s^2}. \quad (7)$$

This simply follows from using polar coordinates. The spacing $p_{\beta,2}(s)$ still needs to be normalised and its first moment set to unity. This is achieved by a rescaling as

$$p_{\beta,2}(s) = \frac{2\alpha^\beta}{\Gamma[1 + \beta/2]} s^{1+\beta} e^{-\alpha s^2}, \quad \alpha = \frac{\Gamma[(3 + \beta)/2]^2}{\Gamma[1 + \beta/2]^2}. \quad (8)$$

This is our first main result for the $N = 2$ 2DCG. It correctly reproduces the 2D Poisson distribution when

setting $\beta = 0$,

$$p_{\text{Poisson}}^{2D}(s) = \frac{\pi}{2} s \exp\left[-\frac{1}{4}\pi s^2\right], \quad (9)$$

which is valid for an infinite number of independent particles, cf. [22]. Second, by construction it agrees with the spacing distribution of the GinUE for $N = 2$ at $\beta = 2$. It is known [8] for any N , in terms of incomplete Gamma functions (or truncated exponentials) as [43]

$$p_{\beta=2,N}(s) = \prod_{j=1}^{N-1} \frac{\Gamma[1+j, s^2]}{\Gamma[1+j]} \sum_{k=1}^{N-1} \frac{2s^{2k+1} e^{-s^2}}{\Gamma[1+k, s^2]}. \quad (10)$$

The limiting distribution is universal, cf. [36, 44]. It is well known [8] that for $N = 2$ eq. (10) is *not* a good approximation to the limiting spacing distribution of the GinUE. This is in sharp contrast to 1D, where $N = 2$ leads to an excellent approximation for $\beta = 2$ (and $\beta = 1, 4$). Therefore, one may expect that away from small β our spacing (8) is not a good approximation at large- N either.

Surmise for Spacing Distribution from β -Ensemble. Let us show how the spacing (8) of a β -ensemble at $N = 2$ can still be used to approximate the spacing distribution of the 2DCG (2) at large- N . The idea here is to apply (8) with an *effective*, improved value of β_{eff} , that is determined by a best fit to the spacing in the 2DCG at a given β . In the comparison we use the library of spacings in the 2DCG that was generated numerically in [13] with $N = 200$ point charges. We have increased this number to $N = 5000$ to improve our Coulomb data in the vicinity of $\beta = 0$. The density of our 2DCG is flat and thus no unfolding is needed. In Fig. 1 we present 4 examples of the best fit of (8) to the 2DCG spacing in a range of $\beta \in [0, 3]$. Although there is a systematic shift in the maximum increasing with β in the approximate, fitted spacing distribution, the description is surprisingly good for this range of values. A comparison between the fitted $\beta_{\text{eff}}(\beta)$ and the true β of the 2D Coulomb data is presented in Fig. 2, taking steps of 0.1 in beta. The curve is very well approximated by a straight line, given by

$$\beta_{\text{eff}}(\beta) = 1.839 \beta. \quad (11)$$

Together with

$$p_{\beta}^{\text{surmise}}(s) = \frac{2\alpha_{\text{eff}}^{\beta}}{\Gamma[1+\beta_{\text{eff}}/2]} s^{1+\beta_{\text{eff}}} \exp[-\alpha_{\text{eff}} s^2], \quad (12)$$

where $\alpha_{\text{eff}} = \frac{\Gamma[(3+\beta_{\text{eff}})/2]^2}{\Gamma[1+\beta_{\text{eff}}/2]^2}$, this is our final *surmise* for the spacing distribution in the 2DCG or non-Hermitian β -ensemble. Although it does not capture the expected repulsion $\sim s^{1+\beta}$ at $s \ll 1$, it describes the overall spacing distribution very well, including its tail.

The standard deviation σ that is used for the fits is shown at the fit points in Fig. 2 and presented in Table

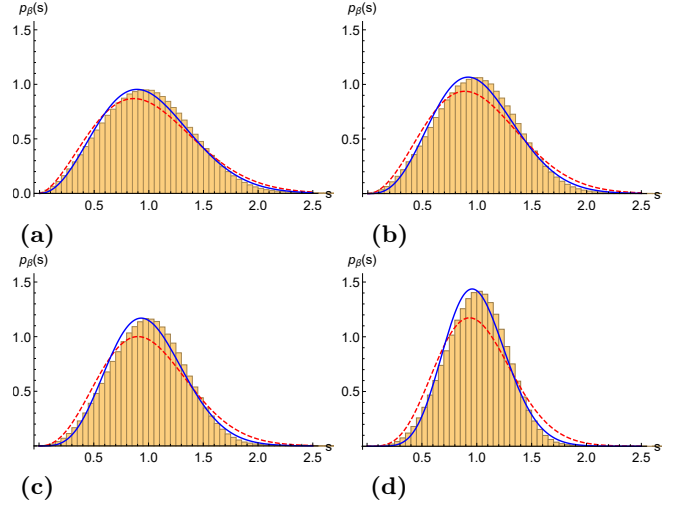


Figure 1. Comparison of 2DCG spacings with $N = 5000$ (histograms) at various values of $\beta = 0.6, 1.0, 1.4, 2.6$ (plots a-d)) with our surmise (12) using (11) for β_{eff} (blue full line). The $N = 2$ result (8) (dashed red line) at the same value β without improvement (11) is not a good approximation.

I. It is defined in the usual way for a chosen β and fitted value $\beta_{\text{eff}}(\beta)$:

$$\sigma = \left[\frac{1}{n} \sum_{j=1}^n (p_{\beta}(s_j) - p_{\beta}^{\text{surmise}}(s_j))^2 \right]^{\frac{1}{2}}, \quad (13)$$

where n is the number of bins in the data and $p_{\beta}(s_j)$ the number of counts in the j -th bin at its mid point s_j . In all data the sum was cut off at $s = 3$, where we have an exponential suppression. To estimate the systematic error for our size of ensemble we have compared matrices from the GinUE of size $N = 5000$ and the 2DCG at the same value $\beta = 2$, leading to $\sigma = 0.44 \cdot 10^{-2}$.

In Table I we also show the Kolmogorov-Smirnov distance d defined as

$$d = \max_{x \geq 0} |F(x) - G(x)| \in [0, 1], \quad (14)$$

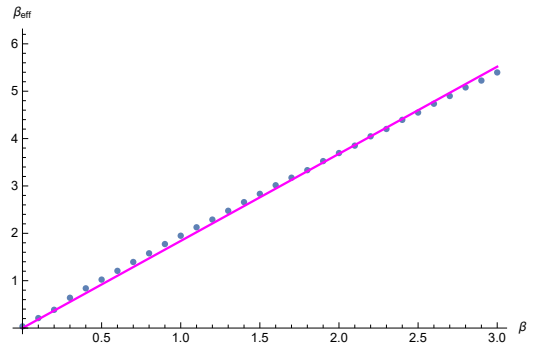


Figure 2. Linear fit of $\beta_{\text{eff}}(\beta)$ (full line).

Table I. List of standard deviations σ and Kolmogorov-Smirnov distances d (both in units 10^{-2}) between surmise (12) and 2DCG, with $\beta \in [0, 3]$ in steps 0.1.

β	0.1	0.2	0.3	0.4	0.5	0.6	0.7	0.8	0.9	1.0	1.1	1.2	1.3	1.4	1.5
σ	0.9	1.6	2.0	2.4	2.7	2.9	3.2	3.5	3.6	3.8	3.9	4.0	4.1	4.2	4.3
d	0.8	0.8	1.1	1.3	1.5	1.6	1.7	1.8	1.9	2.0	2.1	2.1	2.1	2.1	2.2
β	1.6	1.7	1.8	1.9	2.0	2.1	2.2	2.3	2.4	2.5	2.6	2.7	2.8	2.9	3.0
σ	4.4	4.5	4.5	4.6	4.7	4.9	4.9	4.9	4.9	5.2	5.3	5.2	5.2	5.4	5.4
d	2.2	2.3	2.3	2.3	2.3	2.4	2.3	2.3	2.4	2.4	2.4	2.4	2.3	2.4	2.4

between the cumulative distributions F and G of distributions f and g , that is of the spacing distribution of the 2DCG and surmise here. It is independent of the binning into histograms and remains almost constant from $\beta = 1.7 - 3.0$.

In contrast to the Wigner surmise in 1D (1), which becomes a better approximation for increasing values of $\beta = 1$ to $\beta = 4$, but fails when getting closer to 1D Poisson at lower $\beta \rightarrow 0$, we observe the opposite behaviour here. The closer we get to 2D Poisson (9), the better is the approximation, see Tab. I and Fig. 1. Thus when quantifying the transition between integrable (Poissonian) behaviour and fully chaotic random matrix statistics in the respective symmetry class, our surmise may serve as a good parametrisation.

In order to illustrate the usefulness of our surmise we test it on real data from two published works [12, 13] in such an intermediate range for β , and compare with the fit to the 2DCG. In Fig. 3 left, the spacings between occupied nests of the common buzzard in an area of the Teutoburger forrest are shown, where every year serves as a separate ensemble. The β -ensemble is used here as a simple, one-parameter model to quantify the repulsion between these highly territorial birds of prey, see [12] for more discussion. Taking all 3135 data points from the entire period of observation we obtain $\beta = 0.42(0.5)$

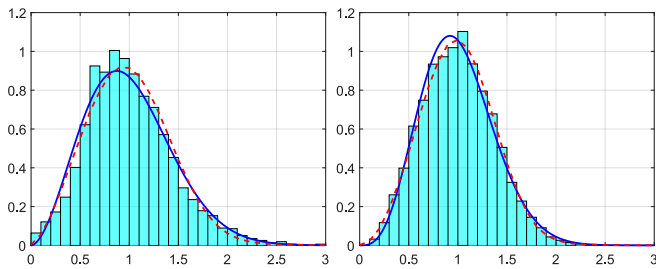


Figure 3. Left: Fit of the spacing distribution between occupied Buzzards nests (histograms) observed annually from 2000-2019 [12] with surmise (12) at $\beta = 0.42$ (red dashed line) and 2DCG at $\beta = 0.5$ (blue full line). Right: Fit of the spacing between the complex eigenvalues of the Liouville operator of an XXX quantum spin chain [13] (histograms) by $\beta = 1(1.05)$ from the 2DCG in blue (surmise in dashed red).

from our surmise (2DCG). In [12] time moving averages of 5 years were used to detect a change in repulsion as measured by β over time, with ≈ 500 data points per time window. On these small sets we have observed similar or larger deviations than 20% in the obtained β -value between the 2DCG and our surmise. Notice however, that the fitted β does not have a biological meaning, but serves as a simple way to quantify time dependence and correlation length in the observed repulsive behaviour.

Fig. 3 right shows a comparison with 77520 spacings of the complex eigenvalues of the Liouville operator of an isotropic Heisenberg XXX spin chain where only the zero-mode is integrable [45], cf. [13] for details of the setup and discussion. Due to the high quality of data a very precise fit of β can be made, that shows very little deviation between surmise and 2DCG. Increasing the parameters responsible for the dissipation in [13] an agreement with the GinUE at $\beta = 2$ (10) was found, which is consistent with fully chaotic behaviour.

Spacing in Class AI^\dagger and AII^\dagger at Non-Integer β . We come to the idea to approximate the spacing distribution of symmetry classes AI^\dagger and AII^\dagger of non-Hermitian random matrices at large- N by a 2DCG with fitted β . Their spacing distributions are unknown beyond $N = 2$ [14, 16], and their large- N limit is conjectured to be universal [14].

For Hermitian random matrices the Dyson index β as it appears in (1) is directly given by the number of independent real degrees of freedom per matrix element. We aim at a precise determination of the fitted values of β in these two non-Hermitian classes AI^\dagger and AII^\dagger for large- N , relying on the 2DCG directly and not our surmise, that loses precision for increasing β .

Figure 4 shows that the spacing distribution of both classes finds an excellent approximation by a 2DCG at *non-integer value* of $\beta = 1.4$ for class AI^\dagger , and $\beta = 2.6$ for class AII^\dagger . We have used step size 0.1 in fitting β . Again unfolding is not needed here as both ensembles have a constant density on the unit disc, see [42] for details.

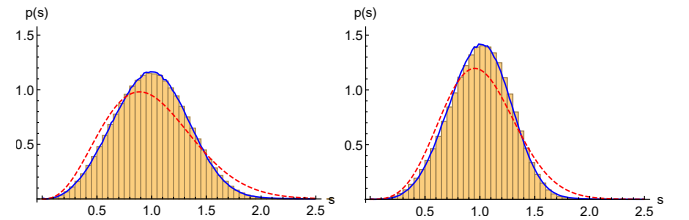


Figure 4. Fit of the spacing distribution of class AI^\dagger with 500 matrices of size $N = 5000$ (histograms) by a 2DCG (blue full line) at $\beta = 1.4$, with $\sigma = 0.86 \cdot 10^{-2}$ and $d = 0.26 \cdot 10^{-2}$ (left). For class AII^\dagger with 500 matrices at $2N = 5000$ (histograms) we obtain $\beta = 2.6$ (blue full line) with $\sigma = 2.29 \cdot 10^{-2}$ and $d = 0.91 \cdot 10^{-2}$ (right). For comparison the analytical results [14, 16] at $N = 2$ (red dashed line) are added (see [42] for details), which do not describe the spacing at large- N well.

Let us emphasise that apart from the spacing distribution so far no further local information about complex eigenvalue correlations in AI^\dagger and AII^\dagger is available. Currently we have no heuristic explanation for the fitted β -values. With the 2DCG description it is easy to compare complex eigenvalue data with a given symmetry class, as it was done for spin chains [14] and the kicked rotor [16], without the need to diagonalise ensembles of large random matrices. In [29] the joint distribution of complex eigenvalues has been obtained for the symmetry class AII^\dagger of complex quaternion self-dual matrices, using a saddle point approximation for large, macroscopic eigenvalues separation. Then it becomes proportional to $|\Delta_N(Z)|^4$, that is a 2DCG at $\beta = 4$, and we see that the local repulsion is very different.

Conclusions. In this letter we have analysed the nearest neighbour spacing distribution in the complex plane resulting from a 2D Coulomb gas at inverse temperature β in a confining potential. We have proposed an invariant matrix representation based on N -dimensional complex normal random matrices. The case $N = 2$ with a Gaussian potential leads us to formulate a surmise, after introducing an effective β_{eff} in a linear fashion. This allowed us to provide a simple measure to study the transition in β between uncorrelated and random matrix statistics in different symmetry classes. The transition has been illustrated by a comparison to spacing distribution from data in a quantum spin chain and ecology. Furthermore, we have established an approximate 2D Coulomb gas description of the spacing distribution in the two symmetry classes of non-Hermitian random matrices AI^\dagger and AII^\dagger at non-integer values of $\beta = 1.4$ and $\beta = 2.6$, respectively, compared to the complex Ginibre ensemble at $\beta = 2$. Although the situation is reminiscent to the 3 classes of Hermitian random matrices with $\beta = 1, 2, 4$, it remains an open problem to explain these non-integer values, and to provide further local spectral information in these two symmetry classes. A further matrix representation for the non-Hermitian β -ensemble, perhaps analogous to the tridiagonal parametrisation of Dumitriu-Edelman in the Hermitian β -ensemble, would be highly desirable to find.

Acknowledgements. This work was funded by the Deutsche Forschungsgemeinschaft (DFG) grant SFB 1283/2 2021 – 317210226 "Taming uncertainty and profiting from randomness and low regularity in analysis, stochastics and their applications" (GA and PP). We thank Mario Kieburg for useful discussions.

* akemann@physik.uni-bielefeld.de

† adm@dtu.dk

‡ patricia@physik.uni-bielefeld.de

[1] O. Bohigas, M.J. Giannoni, and C. Schmit, Phys. Rev. Lett. **52**, 1 (1984); J. Phys. Lett. **45**, 1015 (1984).

- [2] G. Casati, F. Valz-Gris, and I. Guarneri, Lett. Nuovo Cimento **28**, 279 (1980).
- [3] F.J. Dyson, J. Math. Phys. **3**, 1199 (1962).
- [4] T. Guhr, A. Müller-Groeling, and H.A. Weidenmüller, Phys. Rept. **299**, 189 (1998) [arXiv:cond-mat/9707301].
- [5] G. Akemann, J. Baik, and P. Di Francesco (Eds.), *The Oxford Handbook of Random Matrix Theory*, Oxford University Press, Oxford 2011.
- [6] J. Ginibre, J. Math. Phys. **6**, 440 (1965).
- [7] N. Hatano and D.R. Nelson, Phys. Rev. Lett. **77**, 570 (1996) [arXiv:cond-mat/9603165].
- [8] R. Grobe, F. Haake, and H.-J. Sommers, Phys. Rev. Lett. **61**, 1899 (1988).
- [9] H. Sompolinsky, A. Crisanti, and H. J. Sommers, Phys. Rev. Lett. **61**, 259 (1988).
- [10] H. Markum, R. Pullirsch, and T. Wettig, Phys. Rev. Lett. **83**, 484 (1999) [arXiv:hep-lat/9906020].
- [11] B. Ye, L. Qiu, X. Wang, and T. Guhr, Commun. Nonlinear Sci. Numer. Simulat. **20**, 1026 (2015).
- [12] G. Akemann, M. Baake, N. Chakarov, O. Krüger, A. Mielke, M. Ottensmann, R. Werdehausen, J. Theor. Biol. **509**, 110475 (2021) [arXiv:2003.09204].
- [13] G. Akemann, M. Kieburg, A. Mielke, T. Prosen, Phys. Rev. Lett. **123**, 254101 (2019) [arXiv:1910.03520].
- [14] R. Hamazaki, K. Kawabata, N. Kura, M. Ueda, Phys. Rev. Research **2**, 023286 (2020) [arXiv:1904.13082].
- [15] Á. Rubio-García, R.A. Molina, J. Dukelsky, arXiv:2102.13452.
- [16] A.B. Jaiswal, R. Prakash, A. Pandey, EPL **127**, 30004 (2019) [arXiv:1904.12484].
- [17] M. Baus, J.-P. Hansen, Phys. Rep. **59**, 1 (1980).
- [18] A. Alastuey, B. Jancovici, J. Physique **42**, 1 (1981).
- [19] Ph. Choquard, J. Clerouin, Phys. Rev. Lett. **50**, 2086 (1983).
- [20] G. Cardoso, J.-M. Stéphan, A.G. Abanov, J. Phys. A: Math. Theor. **54**, 015002 (2020) [arXiv:2009.02359].
- [21] S. Serfaty, in *Random Matrices*, A. Borodin, I. Corwin, A. Guionnet (Eds.), IAS/Park City Mathematics Series, Volume 26, AMS, Providence (2019), pp. 341-387 [arXiv:1709.04089].
- [22] F. Haake, *Quantum Signatures of Chaos*, 3rd Edition, Springer, Heidelberg (2010).
- [23] R. Grobe, F. Haake Phys. Rev. Lett. **62**, 2893 (1989).
- [24] A. Borodin and C.D. Sinclair, Commun. Math. Phys. **291**, 177 (2009) [arXiv:0805.2986].
- [25] A. Altland, M.R. Zirnbauer Phys. Rev. B **55**, 1142 [arXiv:cond-mat/9602137].
- [26] D. Bernard and A. LeClair, In *Statistical Field Theories*, Springer, Dordrecht, pp. 207-214 (2002) [arXiv:cond-mat/0110649v2].
- [27] U. Magnea, J. Phys. A **41**, 045203 (2008) [arXiv:0707.0418].
- [28] K. Kawabata, K. Shiozaki, M. Ueda, M. Sato, Phys. Rev. X **9**, 041015 (2019) [arXiv:1812.09133].
- [29] M.B. Hastings, J. Stat. Phys. **103**, 903 (2001) [cond-mat/9909234].
- [30] T. Kanazawa, T. Wettig, Phys. Rev. D **104**, 014509 (2021) [arXiv:2104.05846].
- [31] S. Denisov, T. Laptyeva, W. Tarnowski, D. Chruściński, and K. Życzkowski, Phys. Rev. Lett. **123**, 140403 (2019) [arXiv:1811.12282].
- [32] T. Can, J. Phys. A: Math. Theor. **52**, 485302 (2019) [arXiv:1902.01442].

- [33] T. Can, V. Oganessian, D. Ograd, S. Gopalakrishnan, Phys. Rev. Lett. **123**, 234103 (2019) [arXiv:1902.01414].
- [34] L. Sá, P. Ribeiro, T. Prosen, J. Phys. A: Math. Theor. **53**, 305303 (2020) [arXiv:1905.02155].
- [35] P. Vivo, S.N. Majumdar, Physica A **387**, 4839 (2008) [arXiv:0706.2476].
- [36] T. Tao and V. Vu, Ann. Probab. **43**, 782 (2015) [arXiv:1206.1893].
- [37] B. Valkó, B. Virág, Invent. Math. **209**, 275 (2017) [arXiv:1604.04381].
- [38] L. Sá, P. Ribeiro, T. Prosen, Phys. Rev. X **10**, 021019 (2020) [arXiv:1910.12784].
- [39] G. Akemann, S.-S. Byun, J. Stat. Phys. **175**, 1043 (2019) [arXiv:1808.00319].
- [40] M. L. Mehta, *Random Matrices*, Academic Press, 2nd Edition, New York (1990).
- [41] L.-L. Chau, O. Zaboronsky, Commun. Math. Phys. **196**, 203 (1998) [arXiv:hep-th/9711091].
- [42] Supplement to this Letter
- [43] Its first moment still has to be normalised.
- [44] R. Prakash, A. Pandey, EPL **110**, 30001 (2015) [arXiv:1412.6642].
- [45] T. Prosen, Phys. Rev. Lett. **107**, 137201 (2011) [arXiv:1106.2978].

Supplementary Material to:

Spacing distribution in the 2D Coulomb gas: Surmise and symmetry classes of non-Hermitian random matrices at non-integer β

Gernot Akemann,^{1,*} Adam Mielke,^{2,†} and Patricia Păklär^{1,‡}

¹*Faculty of Physics, Bielefeld University, Postfach 100131, 33501 Bielefeld, Germany*

²*Technical University of Denmark, Asmussens Allé, Building 303B, 2800 Kgs. Lyngby, Denmark*
(Dated: April 2, 2022)

* akemann@physik.uni-bielefeld.de

† admi@dtu.dk

‡ patricia@physik.uni-bielefeld.de

Appendix A: Non-Hermitian β -Ensemble at $N = 2$

In this section we provide some details about the non-Hermitian ensemble of Gaussian 2×2 random normal matrices, defined in Eq. (5) in the main text. In particular we will provide an explicit parametrisation, compute the normalisation constants of the distribution of matrix elements and distribution of eigenvalues, before turning to a derivation of the spacing distribution without assuming translational invariance. We also give the spectral density.

1. Definition of the β -Ensemble, Parametrisation and Jacobian

Let us recall the distribution of matrix elements of the non-Hermitian β -ensemble Eq. (5) in the main text, with a Gaussian potential $V(J, J^\dagger) = JJ^\dagger$ for $N = 2$,

$$\mathcal{P}_{\beta, N=2}(J) \propto \frac{\exp[-\text{Tr}(JJ^\dagger)]}{[2\text{Tr}(JJ^\dagger) - \text{Tr}(J)\text{Tr}(J^\dagger)]^\eta}, \quad \eta = 1 - \beta/2 \leq 1. \quad (\text{A1})$$

The normalisation will be determined below. It is not difficult to show that any complex normal 2×2 matrix can be parametrised by the following 6 real parameters, $a_1, a_2, b_1, b_2 \in \mathbb{R}$, $k_1 \in [0, 2\pi)$ and $k_2 \in [0, \infty)$:

$$J = \begin{pmatrix} a & b \\ b^* e^{2ik_1} & a + k_2 e^{ik_1} \end{pmatrix}, \quad a = a_1 + ia_2, \quad b = b_1 + ib_2. \quad (\text{A2})$$

This follows by imposing the condition $[J, J^\dagger] = 0$ onto a complex matrix J and using polar coordinates for certain matrix elements. On the other hand any complex normal matrix can be diagonalised by a unitary transformation U [1], with $U \in U(2)/U(1)^2$ in our case $N = 2$. This can be parametrised as follows, see e.g. [2]:

$$U = \begin{pmatrix} \cos \theta & -e^{-i\phi} \sin \theta \\ e^{i\phi} \sin \theta & \cos \theta \end{pmatrix}, \quad \theta, \phi \in [0, 2\pi). \quad (\text{A3})$$

Thus the diagonalisation reads

$$J = \begin{pmatrix} a & b \\ b^* e^{2ik_1} & a + k_2 e^{ik_1} \end{pmatrix} = U^\dagger \begin{pmatrix} z_1 & 0 \\ 0 & z_2 \end{pmatrix} U, \quad (\text{A4})$$

including the complex eigenvalues $z_1, z_2 \in \mathbb{C}$. As a consistency check this leads to the Jacobian [3]

$$\left| \det \left(\frac{\partial(a, b, k_1, k_2)}{\partial(z_1, z_2, \phi, \theta)} \right) \right| \sim |z_2 - z_1|^2, \quad (\text{A5})$$

for the change of variables (A4). Because the Jacobian from the diagonalisation of J is known to give $|z_2 - z_1|^2$ for $N = 2$, or the absolute value squared of the Vandermonde determinant for general N [4], the parametrisation (A2) can only lead to a constant Jacobian. Together with

$$2\text{Tr}(JJ^\dagger) - \text{Tr}(J)\text{Tr}(J^\dagger) = |z_2 - z_1|^2, \quad (\text{A6})$$

we indeed obtain from (A1) the normalised joint distribution of complex eigenvalues

$$\mathcal{P}_{\beta, 2}(z_1, z_2) = K_\beta |z_2 - z_1|^\beta \exp[-|z_1|^2 - |z_2|^2], \quad K_\beta^{-1} = \pi^2 2^{\beta/2} \Gamma[1 + \beta/2], \quad (\text{A7})$$

of a β -ensemble at $\eta = 1 - \beta/2$, with normalisation constant K_β to be derived below.

2. Normalisation

We compute the normalisation constants C_β and K_β of the distribution of matrix elements and complex eigenvalues, respectively, starting with the former. From the parametrisation (A2), we obtain the following distribution

$$\mathcal{P}_{\beta, 2}(a, b, k_1, k_2) = C_\beta \frac{\exp[-2(|a|^2 + |b|^2 + k_2(a_1 \cos k_1 + a_2 \sin k_1)) - k_2^2]}{[4|b|^2 + k_2^2]^\eta}, \quad C_\eta^{-1} = \frac{\pi^3}{2^{\eta+1/2}} \Gamma\left[\frac{3}{2} - \eta\right], \quad (\text{A8})$$

where we keep the parameter $\eta = 1 - \beta/2$ in the remainder of this section. We need to show that its integral is normalised:

$$1 = \int_0^{+\infty} dk_2 \int_0^{2\pi} dk_1 \int_{\mathbb{C}} d^2a \int_{\mathbb{C}} d^2b \mathcal{P}_{\beta,2}(a, b, k_1, k_2). \quad (\text{A9})$$

The integration can be done in several steps, using that some of the integrals factorise. We start with the integration over b and choose polar coordinates. Using [5, 3.382(4)], we obtain

$$\int_{\mathbb{C}} d^2b \frac{\exp[-2|b|^2]}{[4|b|^2 + k_2^2]^\eta} = \pi 2^{-1-\eta} \exp\left[\frac{k_2^2}{2}\right] \Gamma\left[1 - \eta, \frac{k_2^2}{2}\right], \quad (\text{A10})$$

where $\Gamma[x, y] = \int_y^\infty t^{x-1} e^{-t} dt$ is the incomplete gamma function. The integrations over $a = a_1 + ia_2$ are simple shifted Gaussian integrals, leading to

$$\int_{-\infty}^{+\infty} da_1 \int_{-\infty}^{+\infty} da_2 \exp[-2(a_1^2 + a_2^2 + k_2(a_1 \cos k_1 + a_2 \sin k_1))] = \frac{\pi}{2} \exp\left[\frac{k_2^2}{2}(\cos^2(k_1) + \sin^2(k_1))\right]. \quad (\text{A11})$$

Consequently, the k_1 -dependence drops out and integrating over k_1 yields 2π . We are left with the integral over k_2 where the exponentials cancel, leading to

$$C_\beta^{-1} = \pi^3 2^{-1-\eta} \int_0^\infty dk_2 \Gamma\left[1 - \eta, \frac{k_2^2}{2}\right] = \pi^3 2^{-1-\eta} \sqrt{2} \Gamma\left[\frac{3}{2} - \eta\right]. \quad (\text{A12})$$

This step follows from [5, 6.455(1)] and we arrive at the result claimed in (A8).

For the normalisation K_β of the joint probability density of complex eigenvalues we have to show

$$1 = K_\beta \int_{\mathbb{C}} d^2z_1 \int_{\mathbb{C}} d^2z_2 e^{-(|z_1|^2 + |z_2|^2)} |z_2 - z_1|^{2-2\eta}. \quad (\text{A13})$$

We change variables $(z_1, z_2) \rightarrow (z_1, z)$ with $z = z_2 - z_1$, and choose polar coordinates as $z_1 = r_1 e^{i\Theta_1}$ and $z = r_2 e^{i\Theta_2}$. After this transformation, we find

$$K_\beta^{-1} = \int_0^{2\pi} d\Theta_1 \int_0^\infty dr_1 r_1 \int_0^{2\pi} d\Theta_2 \int_0^\infty dr_2 r_2^{3-2\eta} \exp[-2r_1^2 - r_2^2 - 2r_1 r_2 \cos(\Theta_1 - \Theta_2)]. \quad (\text{A14})$$

After using an addition theorem for cosine, one of the angular integration can be done employing [5, 3.338(4)]:

$$\int_0^{2\pi} d\Theta_1 \exp[b \sin \Theta_1 + c \cos \Theta_1] = 2\pi I_0(y) \quad \text{with } y = \sqrt{b^2 + c^2} = 2r_1 r_2. \quad (\text{A15})$$

Here $I_0(y)$ denotes the modified Bessel function of the first kind. The second angular integral then becomes trivial, giving 2π , and we have

$$K_\beta^{-1} = (2\pi)^2 \int_0^\infty dr_1 r_1 \int_0^\infty dr_2 r_2^{3-2\eta} \exp[-2r_1^2 - r_2^2] I_0(2r_1 r_2). \quad (\text{A16})$$

The integral over r_1 follows using [5, 6.631(4)]:

$$\int_0^\infty dr_1 r_1 \exp[-2r_1^2] I_0(2r_1 r_2) = \frac{1}{4} e^{r_2^2/2}. \quad (\text{A17})$$

For the remaining integral over r_2 we thus obtain

$$K_\beta^{-1} = \pi^2 \int_0^\infty dr_2 r_2^{3-2\eta} \exp[-r_2^2/2] = \pi^2 2^{1-\eta} \Gamma(2 - \eta), \quad (\text{A18})$$

as was claimed in (A7), after inserting $\eta = 1 - \beta/2$.

3. Spacing Distribution and Spectral Density

Let us first derive the nearest-neighbour spacing distribution in radial distance, $p_{\beta,2}(s)$, Eq. (7) in the main text. There it was argued, that using translational invariance we may put one eigenvalue at the origin, $z_1 = 0$, and then compute the probability that the next eigenvalue z_2 is located at radius s . Here, we will show that the same result holds when using the proper definition of the spacing distribution for $N = 2$,

$$p_{\beta,2}(s) = \int_{\mathbb{C}} d^2 z_1 \int_{\mathbb{C}} d^2 z_2 P_{\beta,2}(z_1, z_2) \delta(s - |z_2 - z_1|). \quad (\text{A19})$$

It describes the probability to find the two eigenvalues at distance s from another, where here there are no further eigenvalues present. Using the very same change of variables from the previous subsection (A14), we obtain

$$\begin{aligned} p_{\beta,2}(s) &= K_{\beta} \int_0^{2\pi} d\Theta_1 \int_0^{\infty} dr_1 r_1 \int_0^{2\pi} d\Theta_2 \int_0^{\infty} dr_2 r_2^{3-2\eta} \exp[-(2r_1^2 + r_2^2 + 2r_1 r_2 \cos(\Theta_2 - \Theta_1))] \delta(s - r_2) \\ &= K_{\beta} \pi^2 s^{3-2\eta} e^{-s^2/2}. \end{aligned} \quad (\text{A20})$$

Because we can follow the same steps of integration we just give the final answer here. It is easy to check that it is indeed properly normalised. However, we still need to rescale the first moment to unity, which reads

$$m = \int_0^{\infty} ds s p_{\beta,2}(s) = 2^{\frac{1}{2}} \frac{\Gamma(\frac{5}{2} - \eta)}{\Gamma(2 - \eta)}. \quad (\text{A21})$$

Thus our final answer for the spacing distribution with normalised first moment is

$$\hat{p}_{\beta,2}(s) = m p_{\beta,2}(ms) = \frac{2\alpha^{2-\eta}}{\Gamma(2-\eta)} s^{3-2\eta} \exp[-\alpha s^2], \quad \text{with } \alpha = \frac{\Gamma(\frac{5}{2} - \eta)^2}{\Gamma(2 - \eta)^2}. \quad (\text{A22})$$

It agrees with the quantity given in Eq. (8) in the main text, after dropping the hat and inserting $\beta = 2 - 2\eta$.

Figure 1 left shows the normalised nearest neighbour spacing distribution $p_{\beta,2}(s)$ (A22) for several values of the inverse temperature β . The red bottom curve is the spacing distribution of the 2D Poisson ensemble at large N [2],

$$p_{\text{Poisson}}^{2D}(s) = \frac{\pi}{2} s \exp\left[-\frac{1}{4}\pi s^2\right], \quad (\text{A23})$$

which is obtained by setting $\beta = 0$ in (A22), and the blue top curve of the complex Ginibre ensemble [6, 7] at $N = 2$ obtained by setting $\beta = 2$ in (A22). It follows from Eq. (10) given for general N in the main text

$$p_{\beta=2, N=2}(s) = 2s^3 \exp[-s^2], \quad (\text{A24})$$

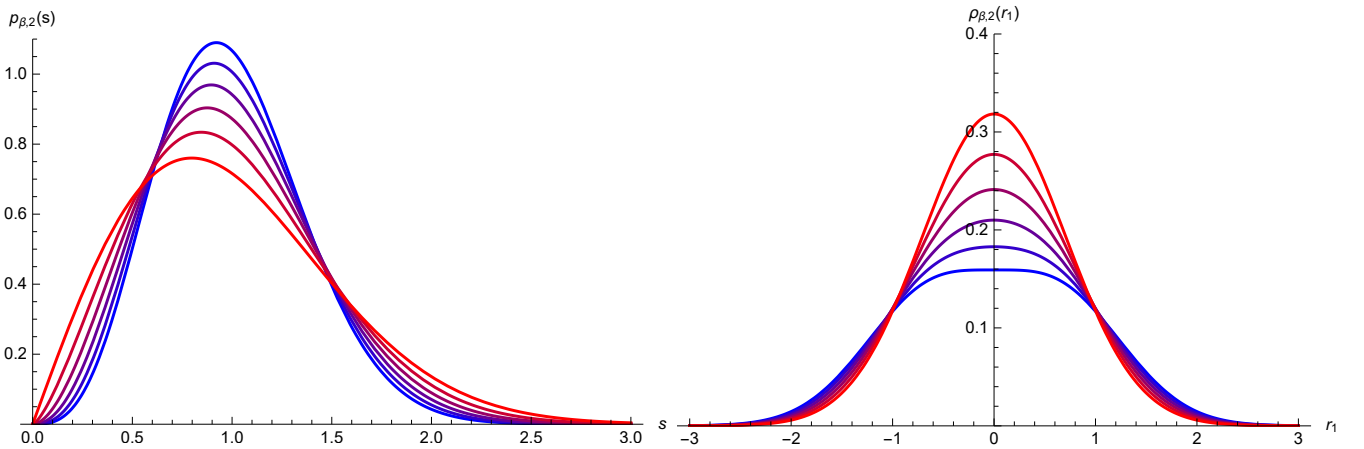


Figure 1. Left: spacing distribution $p_{\beta,2}(s)$ (A22) for several values of $\beta = 0, 0.4, 0.8, 1.2, 1.6$ and 2 , where the blue top curve corresponds to $\beta = 2$ (complex Ginibre) and the red bottom curve to $\beta = 0$ (2D Poisson). Right: spectral density $\rho_{\beta,2}(r_1)$ at the same values of β from (A27). Here the red top curve represents Poisson and the blue bottom curve the complex Ginibre ensemble.

after normalising its first moment

$$m_2 = \int_0^\infty ds s p_{2,2}(s) = \sqrt{\pi} \frac{3}{4}, \quad (\text{A25})$$

to unity by rescaling as in (A22). We observe that the probability that the two eigenvalues coincide always vanishes as $p_{\beta,2}(s) \sim s^{1+\beta}$. Increasing β from 0 to 2 the maximum increases and is shifted to the right.

Let us turn to the spectral density $\rho_{\beta,2}(z_1)$ which is defined as

$$\rho_{\beta,2}(z_1) = \int_{\mathbb{C}} dz_2 P_{\beta,2}(z_1, z_2). \quad (\text{A26})$$

In our convention it is normalised to unity. We can again follow the same lines as in the determination of the normalisation constant K_β above, by changing variables $z_2 \rightarrow z = z_2 - z_1 = r_2 e^{i\Theta_2}$ as in (A14). The outcome will be rotation invariant, only depending on $|z_1| = r_1$. We first integrate over the angle Θ_2 to obtain

$$\begin{aligned} \rho_{\beta,2}(z_1) &= K_\beta 2\pi e^{-2r_1^2} \int_0^\infty dr_2 r_2^{1+\beta} e^{-r_2^2} I_0(2r_1 r_2) \\ &= \frac{1}{2^{\beta/2} \pi} \exp[-2r_1^2] {}_1F_1(1 + \beta/2; 1; r_1^2). \end{aligned} \quad (\text{A27})$$

Here, ${}_1F_1(a; b; x)$ is Kummer's hypergeometric function, and in the last step we have applied [5, 6.631(1)], inserted K_β and cancelled common factors. At the special values $\beta = 2$ (complex Ginibre), respectively $\beta = 0$ (Poisson) we obtain for the density of our $N = 2$ β -ensemble

$$\rho_{\beta=2,2}(r_1) = \frac{1}{2\pi} (1 + r_1^2) \exp[-r_1^2], \quad (\text{A28})$$

$$\rho_{\beta=0,2}(r_1) = \frac{1}{\pi} \exp[-r_1^2]. \quad (\text{A29})$$

This follows from the Taylor series

$${}_1F_1(a; b; x) = 1 + \frac{a}{b}x + \frac{a(a+1)}{b(b+1)2!}x^2 + \dots, \quad (\text{A30})$$

and the connection formula [8, 13.2.39]

$${}_1F_1(a; b; x) = e^x {}_1F_1(b - a; b; -x), \quad (\text{A31})$$

at $a = 2, b = 1$ and $a = b = 1$, respectively.

The right diagram in Figure 1 shows the spectral density (A27) for several values of the inverse temperature β . Because $\rho_{\beta,2} = \rho_{\beta,2}(|z_1| = r_1)$ is rotationally invariant we only show 1D cuts. The two special cases $\beta = 2$ and $\beta = 0$ are represented by the blue bottom and the red top curve, respectively. For $\beta = 2$ the beginning of the formation of a plateau of a constant density on the unit circle can be seen, the circular law, which is known to hold in the large- N limit of the Ginibre ensemble (and many other non-Hermitian ensembles, cf. [9, Ch. 18]). The two-dimensional (2D) Gaussian density in the case of Poisson random variables is also well known.

Appendix B: Comparison of Classes AI^\dagger and AII^\dagger with 2D Coulomb Gas at $N = 2$ and Large- N

The goal of this section is to introduce the symmetry classes AI^\dagger and AII^\dagger of Gaussian random matrices following the nomenclature of [10], and to compare them with the spacing distribution of the non-Hermitian β -ensemble also called 2D Coulomb gas (2DCG), given by Eq. (2) in the main text. To begin with, at $N = 2$ we have analytical expressions at hand to do the fit. We will then explain how the fit is made comparing large- N simulation of classes AI^\dagger and AII^\dagger to the 2DCG. Here, we will not use the surmise from the previous section A but use directly the 2DCG. This is because we aim at the most accurate determination of the fitted value of β , that turns out to be non-integer valued.

1. Definition of Classes AI^\dagger and AII^\dagger and Analytic Results for $N = 2$

We begin with recalling the definition of the complex Ginibre ensemble (GinUE) [6]. It is given by the complex matrices $J \in \mathbb{C}^{N \times N}$ of size N without further constraint, in particular $J \neq J^\dagger$, that have the following Gaussian distribution of matrix elements

$$\mathcal{P}_{2,N}(J) \propto \exp[-\text{Tr}(JJ^\dagger)]. \quad (\text{B1})$$

Class AI^\dagger is defined by all *complex symmetric* matrices, that is $J \in \mathbb{C}^{N \times N}$ with the constraint

$$\text{class } \text{AI}^\dagger : J = J^T, \quad (\text{B2})$$

with the same distribution of matrix elements (B1). Finally class AII^\dagger is given by all *complex quaternion* matrices of size N that are self dual, with distribution (B1). If we choose the complex representation of such matrices of size $2N$, the self-duality can be written as follows

$$\text{class } \text{AII}^\dagger : J = \Sigma J^T \Sigma, \quad (\text{B3})$$

with the skew metric

$$\Sigma = \begin{pmatrix} 0 & -i1_{N \times N} \\ i1_{N \times N} & 0 \end{pmatrix}. \quad (\text{B4})$$

It was pointed out in [11] that this ensemble can be realised by antisymmetric complex matrices $A = -A^T$ via $J = i\Sigma A$, and in that sense these two ensembles are related. As far as we are aware of no results are known to date about the joint densities of complex eigenvalues of classes AI^\dagger and AII^\dagger , including for $N = 2$. Using a saddle point approximation it was shown in [11] that for large eigenvalue separation AII^\dagger is approximately described by a 2DCG at $\beta = 4$.

For $N = 2$, starting from the matrix representation the spacing distribution could be computed analytically [10], see also [12] for AI^\dagger :

$$p_{\text{AI}^\dagger, N=2}(s) = 2C_{\text{AI}^\dagger}^4 s^3 K_0(C_{\text{AI}^\dagger}^2 s^2), \quad (\text{B5})$$

$$p_{\text{AII}^\dagger, N=2}(s) = \frac{2}{3}C_{\text{AII}^\dagger}^4 s^3 (1 + C_{\text{AII}^\dagger}^2 s^2) \exp[-C_{\text{AII}^\dagger}^2 s^2], \quad (\text{B6})$$

where $C_{\text{AI}^\dagger} = \Gamma[1/4]^2/2^{7/2}$ and $C_{\text{AII}^\dagger} = 7\sqrt{\pi}/8$. They are normalised including their first moment and shown in Fig. 2. Here $K_0(x)$ denotes the modified Bessel-function of the second kind $K_0(x)$. Notably for class AI^\dagger it was used in [12] that the two complex eigenvalues can be computed explicitly in terms of the matrix elements J_{kl} , yielding the expression $s = |z_2 - z_1| = \sqrt{[(J_{11} - J_{22})^2 - 4J_{12}J_{21}]}$. Compared to the spacing in the GinUE at $N = 2$ (A24), class

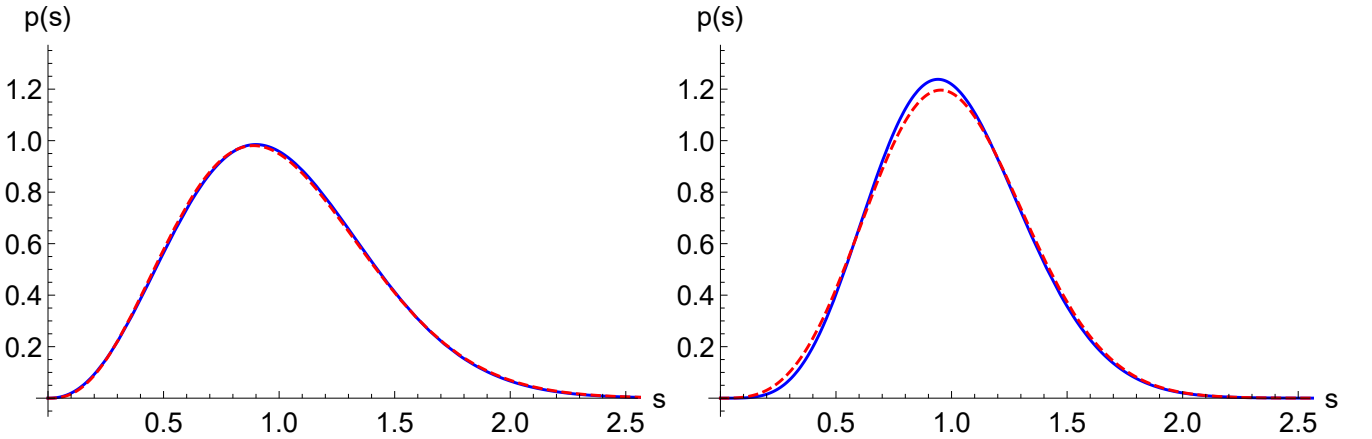


Figure 2. Comparison of the spacing distribution at $N = 2$ for class AI^\dagger (B5) (red dashed line) with the β -ensemble (A22) (blue full line) at $\beta = 1.3$ with standard deviations $\sigma = 0.57 \cdot 10^{-2}$ (left), and class AII^\dagger (B6) (red dashed line) with (A22) (blue full line) at $\beta = 2.8$ with $\sigma = 1.16 \cdot 10^{-2}$. The first moment of all spacings is normalised to unity.

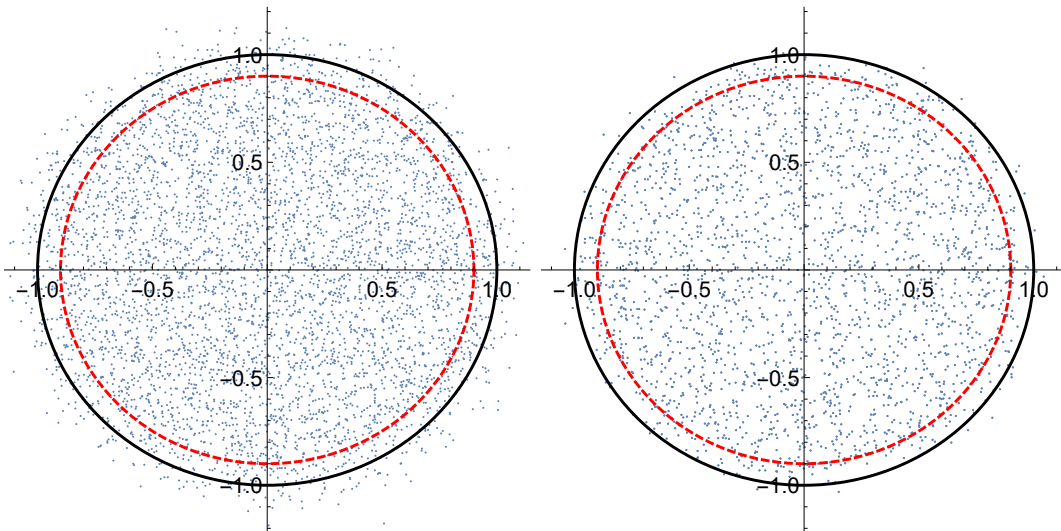


Figure 3. Scatterplot of complex eigenvalues of 50 complex symmetric matrices of size $N = 100$ (left), and of 50 complex quaternion self-dual matrices of size $2N = 100$ (right), where every eigenvalue (point) is doubly degenerate. To ensure that we probe only the bulk statistics of the spacing distributions the spacings among eigenvalues inside the red rings are used. Its radius is chosen approximately at equal distance from the limiting support (black curve) as the eigenvalues lying outside of it. Both averaged densities can be seen to be constant inside the considered region.

AII^\dagger in (B6) shares the same cubic repulsion $\sim s^3$ at $s \ll 1$. This feature was shown in [2] to hold universally for a large class of ensembles at large- N , using perturbation theory. In contrast, due to the logarithmic singularity at the origin in (B5), $K_0(x) \sim -\ln(x)$ for $x \ll 1$, class AI^\dagger behaves rather as $\sim s^3 \ln(s)$. All three spacing distribution have Gaussian tails, due to $K_0(x) \sim \sqrt{\pi/(2x)}e^{-x}$ for $x \gg 1$ [8, 10.25.3]. Let us emphasise that, as it is already known for the GinUE [17], neither (B5) nor (B6) at $N = 2$ provide good approximations for the respective limiting spacing distributions, see Fig. 4 below.

As a first step, let us see if the analytical results (B5) and (B6) at $N = 2$ can be approximated by our spacing distribution $p_{\beta,2}(s)$ of a 2DCG also at $N = 2$, by fitting β as shown in Fig. 2. Despite the different logarithmic behaviour at very small spacing for class AI^\dagger , the approximation with non-integer values of β is excellent for this class. The precise values of the fitted β are not so important here, as we are not yet in the large- N limit which is supposed to be universal [10]. As we have seen in the main text, such an approximation by a 2D Coulomb gas pertains also there, as explained now.

2. Comparison of Classes AI^\dagger and AII^\dagger at Large N

We turn to the fit of the spacing distributions at large- N by comparing to the 2DCG directly. In Fig. 3 scatterplots of numerically generated random matrices in the ensembles AI^\dagger (left) and AII^\dagger (right) as defined above are shown for illustration. In each case the complex eigenvalues of 50 random matrices of size 100 each are averaged over, and we observe several properties of the resulting spectral density. In both cases the density is approximately constant, concentrated on the unit disc. This property called the circular law holds for a large class of ensembles, including the 2DCG at fixed $\beta > 0$ (when the factor β is again included in the Gaussian potential (B1), cf. [14]). Second, the eigenvalues slightly spread outside the limiting unity disc, an effect more pronounced for ensemble AI^\dagger . Finally, apparently no complex conjugation symmetry is present, neither do real eigenvalues play a distinct role here, as it is the case among the three Ginibre ensembles.

Because the density is constant in both cases, see Fig. 3, no unfolding is needed here, see [2, 15, 16] for a discussion of this issue. Second, as it is well known from the complex Ginibre ensemble [17], the correlations among eigenvalues change close to the edge compared to the bulk. Thus, in order to probe bulk statistics, we only consider the spacing among eigenvalues within the red ring of distance (the nearest neighbour may lie outside the red ring though). For the generation of the spacing distribution of the classes AI^\dagger and AII^\dagger we considered 500 random matrices of size $N = 5000$, respectively $2N = 5000$. The resulting histograms are shown in Fig. 4 below which reproduces Fig. 4 from the main text for completeness. The red curves show the corresponding spacing distributions (B5) and (B6) at $N = 2$, which clearly do not approximate the spacing at large- N well. The best fit to the 2DCG is shown by the blue

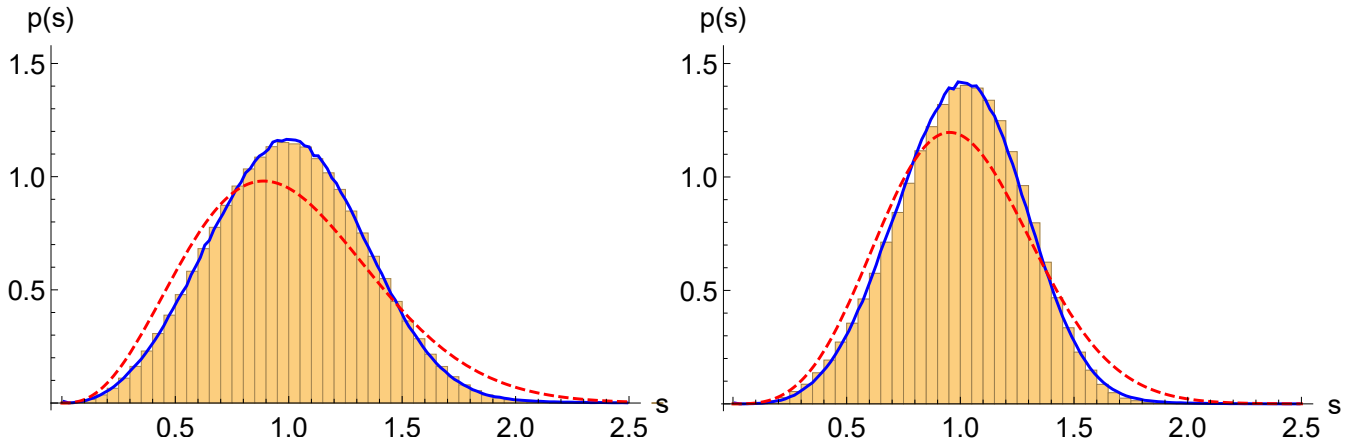


Figure 4. Comparison of the spacing distribution $p(s)$ of complex eigenvalues for 500 matrices of size $N = 5000$ for class AI^\dagger (B5) (red dashed line) with the 2DCG (blue full line) at $\beta = 1.4$ (left), and class AII^\dagger (B6) (red dashed line) with the 2DCG (blue full line) at $\beta = 2.6$ (right). The first moment of all spacings is normalised to unity.

curve, which described both tails and the global maximum well. We use the approach presented in [15] and extended the 2DCG to $N = 5000$ points as well, to improve our precision.

In Fig. 5 we illustrate our fit by plotting the standard deviation σ and Kolmogorov-Smirnov distance d defined in the main text in Eqs. (13) and (14), obtained at different values of β of the 2DCG, in step size 0.1. The best fit indicated by the local minimum agrees for both measures of distance. From the plots it seems that the closest half integer values of $\beta = 1.5$ for AI^\dagger and of $\beta = 2.5$ for AII^\dagger are disfavoured. We should keep in mind however, that the fit by the 2DCG is an effective description of the otherwise unknown local statistics in these two symmetry classes.

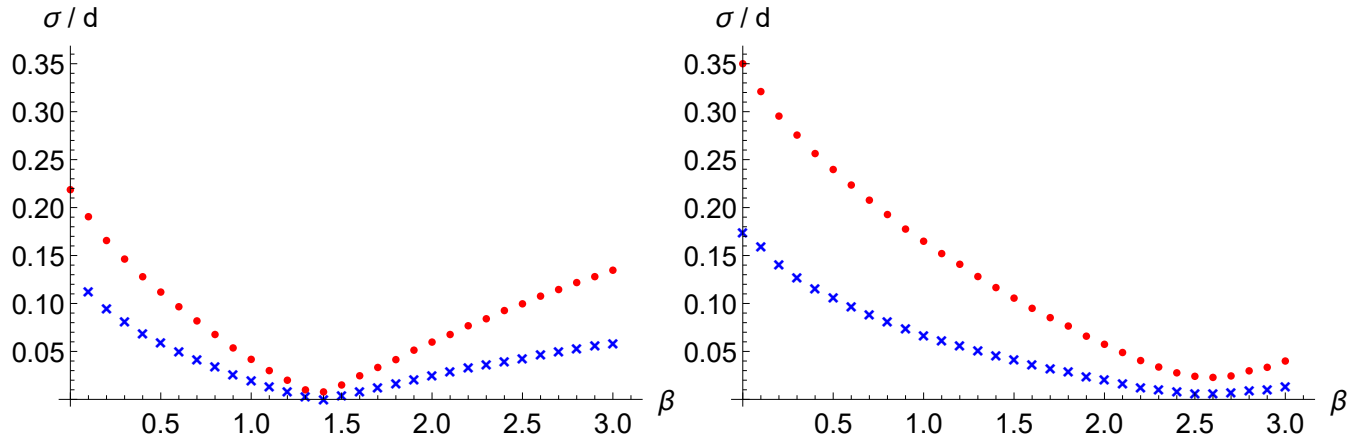


Figure 5. Standard deviation σ (red dots) and Kolmogorov-Smirnov distances d (blue crosses) between the 2DCG data at different values of $\beta \in [0, 3]$, and the bulk spacings for random matrices of class AI^\dagger (left) and AII^\dagger (right) as shown in Fig. 4.

-
- [1] G. H. Golub, and C. F. van Loan, *Matrix Computations*, The Johns Hopkins University Press, 4th ed. (2013), Baltimore.
 - [2] F. Haake, *Quantum Signatures of Chaos*, 3rd Edition, Springer, Heidelberg (2010).
 - [3] P. Päsler, *On Non-Hermitian Beta-Ensembles*, Master thesis Bielefeld University, September 2021.
 - [4] L.-L. Chau, O. Zaboronsky, Commun. Math. Phys. **196**, 203 (1998) [arXiv:hep-th/9711091].
 - [5] I. S. Gradshteyn, *Table of Integrals, Series, and Products*, Academic Press, 6th ed. (2000), San Diego.
 - [6] J. Ginibre, J. Math. Phys. **6**, 440 (1965).
 - [7] M. L. Mehta, *Random Matrices*, Academic Press, 2nd Edition, New York (1990).
 - [8] F.W.L Olver et al. (eds.), NIST Handbook of Mathematical Functions. Cambridge University Press, Cambridge 2010.

- [9] G. Akemann, J. Baik, and P. Di Francesco, *The Oxford Handbook of Random Matrix Theory*, Oxford University Press, (2011), Oxford.
- [10] R. Hamazaki, K. Kawabata, N. Kura, M. Ueda, Phys. Rev. Research **2**, 023286 (2020), [arXiv:1904.13082].
- [11] M.B. Hastings, J. Stat. Phys. **103**, 903 (2001) [cond-mat/9909234].
- [12] A.B. Jaiswal, R. Prakash, A. Pandey, EPL **127**, 30004 (2019) [arXiv:1904.12484].
- [13] R. Grobe, F. Haake Phys. Rev. Lett. **62**, 2893 (1989).
- [14] S. Serfaty, in *Random Matrices*, A. Borodin, I. Corwin, A. Guionnet (Eds.), IAS/Park City Mathematics Series, Volume 26, AMS, Providence (2019), pp. 341-387 [arXiv:1709.04089].
- [15] G. Akemann, M. Kieburg, A. Mielke, T. Prosen, Phys. Rev. Lett **123**, 254101 (2019) [arXiv:1910.03520].
- [16] H. Markum, R. Pullirsch, and T. Wettig, Phys. Rev. Lett. **83**, 484 (1999) [arXiv:hep-lat/9906020].
- [17] R. Grobe, F. Haake, and H.-J. Sommers, Phys. Rev. Lett. **61**, 1899 (1988).